Supporting Information

Tomassy et al. 10.1073/pnas.0911792107

SI Methods

Immunocytochemistry and In Situ Hybridization. For protein detection, the following primary antibodies were used: rabbit anti-COUP-TFI (1:500) (1), rabbit anti-Tbr1 (1:1000, gift from R. Hevner), rat anti-CTIP2 (1:500, Abcam), mouse anti-BrdU (1:300, Sigma), rabbit anti-FOXP2 (1:2000, Abcam), and mouse anti-GFP. The following secondary antibodies were used: 1:400, Alexafluor 488 α-rabbit; Alexafluor 594 α-rabbit; Alexafluor 594 α-mouse (Molecular probes). For transcript detection, the following probes were used: *COUP-TFI* (gift of M. Tsai); *Fezf2*, *Crim1*, *Igfbp4*; and *Tbr1* (gift of R. Hevner).

Behavioral Analysis. ***General.*** For the behavioral studies, 26 *WT* and 16 *COUP-TFI CKO* mice, which were matched for gender (*WT*: 14 males and 12 females; *COUP-TFI CKO*: 8 males and 8 females) and age (*WT*: 81.6 ± 5.1; *COUP-TFI CKO*: 96.9 ± 14.2 days) were used in total. Mice were placed, individually or grouped (about 2–3), in standard breeding cages, in a rearing room at a constant temperature (22 ± 2°C), and maintained on a 12-h light/dark cycle with food and water available ad libitum. The behavioral testing room had constant sound and light background. Animals were tested during their light phase, between 9:00 AM and 5:00 PM. Before each behavioral task, animals were acclimatized to the testing room for at least 30 min. Before each testing, mice were placed in a waiting cage for at least 10 min before the beginning of the task; at the end of the measurement, they were placed back in their home cage.

Details and results. In the adhesive patch removal task, sensorial perception status was measured by measuring the latency (s) to the first contact of one of the two patches for the first trial. Skilled patch removal ability was measured by calculating the Percentage Success = (number of patches removed in the three trials/6)/100 and number of nose contact with each patch. Although the two-way ANOVA for repeated measures on the percentage of success revealed an almost significant effect of trials ($F_{2/38} = 3.205$; $P = 0.051$), posthoc test demonstrated that *COUP-TF1 CKO* animals did not improve their performance from trial 1 to trial 3 ($P = 0.54$). Consequently, as indicated by the highly significant effect of the variable trials ($F_{2/38} = 13.961$; $P < 0.0001$), they decreased the number of contacts across trials ($P = 0.0005$), once found that their attempts were unsuccessful.

In the skilled reaching task, a plexiglass reaching box (19.5-cm long, 8-cm wide, 20-cm high) was used. A 1-cm wide vertical slit ran up the front of the box. A 0.2-cm thick shelf (8.3-cm long and 3.8-cm wide) was mounted 1.1 cm from the floor on the front of the box. Chocolate flavored rice crisps were placed in the indentation. Mice were isolated and food deprived until they reached 85% of their normal weight, then habituated to the chocolate pellets in their home cage during the 3 days before starting the test.

The task consisted of three phases: habituation, unskilled reaching, and skilled reaching. Two consecutive (ITI = 2 h) habituation trials were performed on day 1, in which the mice were placed in the testing cage with 10 pellets scattered on the floor; the trial ended when all of the pellets were eaten or 10 min passed. Two consecutive (ITI = 2 h) unskilled reaching trials were performed for 2 consecutive days (day 2 and 3), in which pellets were available on the shelf within reach of their tongue distance; mice retrieved them one by one. The trial ended when 10 pellets were retrieved or 10 min passed. After 2 days of rest, the skilled reaching single trial was performed for 2 consecutive days. Pellets were placed in both indentations, allowing mice to use their forelimb paws. The trials ended when 20 pellets were retrieved or displaced to an unreachable distance, or when 10 min elapsed. Filming was done during the unskilled and skilled trials, with a Panasonic WV-BP332 CCTV camera (Stoelting). Animals were filmed on a frontal view. Food retrieval either on the shelf (during the unskilled reaching trial) or on the tray (during the skilled trial) was scored as a success. If the animal knocked the food away, the reach was scored as a miss. Performance was defined by: Percent Success = (number of successful retrieval/20)/100.

Two-way ANOVA for repeated measures on the percentage of success in the skilled reaching task, demonstrated no significant effect of the variable group per se ($F_{1/15} = 0.986$; $P = 0.336$), but highly significant effect of the testing phase ($F_{1/15} = 208.845$; $P < 0.0001$) and of the interaction between the two variables ($F_{1/15} = 16.994$; $P = 0.0009$) (Fig. 6 *D* and *E*).

Behavior. General motor activity and behavior were studied in the activity cage for 5 min, and measured using a video-tracking system. No significant differences in the distance traveled ($F_{1/20} = 2.131$; $P = 0.16$) (Fig. S9*A*) or the mean speed ($F_{1/20} = 2.236$; $P = 0.15$) (Fig. S9*B*). A trained observer scored off-line rearing (time standing on the hindlimbs), self-grooming, and leaning (time standing on the hindlimbs while placing the forelimbs on the wall of the activity cage). There were no significant differences between the two groups in rearing ($F_{1/20} = 0.635$; $P = 0.435$) (Fig. S9*C*), leaning ($F_{1/20} = 3.421$; $P = 0.079$) (Fig. S9*D*), or self-grooming time ($F_{1/20} = 0.068$; $P = 0.797$) (Fig. S9*E*). No significant differences in basic neuromuscular function were detected in *COUP-TFI CKO* mice compared to *WT* mice using the hanging wire test, which measures the ability of the mice to hang upside down on a wire ($F_{1/14} = 2.217$; $P = 0.15$) (Fig. S9*F*). Pure motor coordination was measured using the rotarod test, which measures the ability of mice to use a coordinated walking pattern to hang on to an accelerating rod; this performance is thought to be substantially also mediated by the cerebellum. There were no significant differences in rotarod performance between *WT* and *CKO* mice [group ($F_{1/15} = 0.06$; $P = 0.800$); trials ($F_{2/30} = 0.995$; $P = 0.382$), and group × trial ($F_{2/30} = 0.221$; $P = 0.803$)] (Fig. S9*G*). These data strongly suggest that *COUP-TFI CKO* mice have no basic motor weakness or function that would explain nonspecific defects in skilled sensorimotor behavior in the patch removal (Fig. 6 *A–C*) and skilled reaching (Fig. 6 *D–G'*) tasks.

Experimental Procedures. ***General motor functions tasks.*** General motor activity was measured in an activity cage, with metal floor and plexiglass transparent walls, covered with white paper. At the beginning of the measurement, each mouse was released from the center of the activity cage. Mice were tested for 5 min, during which a video-tracking system (ANY-MAZE) calculated the total distance traveled (m), the speed (m/s). Self-grooming time (grooming directed to the mouse's body) and vertical activity, distinguished by leaning (standing on the hindlimbs with both forelimbs on the wall) and rearing time (standing on the hindlimbs with no support for the forelimbs), were also analyzed. The analysis was manually done off-line by a trained observer blind to the genotype of the mice. Neuromuscular strength was tested by the hanging-wire test. Mice were placed on a wire cage lid and the lid was gently waved so the mice gripped the wire lid. The lid was then turned upside down. Latency to fall off the lid was recorded, with a cut-off time of 60 s. Motor coordination was tested by using the rotarod apparatus for mice (Ugo Basile) with five rods. Each mouse was gently placed on each rod set at a

steady slow speed of 5 rpm. The trial started when all mice moved in the right direction. The rotarod was set at increasing speeds ranging from 5 to 40 rpm over 5 min. The latency to fall off the rotarod within this period was recorded. Three consecutive trials were performed, with an ITI of 15 min.

Statistical analysis. One-way ANOVA with a between-group factor genotype (two levels: *WT*, *COUP-TFI CKO*) was used to analyze the latency to first contact the patch in the patch removal task; the distance, speed, leaning time, rearing time, and self-grooming time in the activity cage; and the latency to fall off the grid in the hanging wire test. A two-way ANOVA for repeated measures with a between-group factor genotype (two levels: *WT*, *COUP-TFI CKO*), and testing trials (three levels: T1, T2, and T3) as repeated measures, was used to analyze the percentage of success, the removal time, the number of contacts in the patch removal task, and the fall-off latency in the rotarod task. A two-way ANOVA for repeated measures with a between-group factor genotype (two levels: *WT*, *COUP-TFI CKO*) and testing phase (two levels: unskilled reaching and skilled reaching) was used to analyze the percentage of success in the skilled reaching task. The Tukey Honestly Significant Difference post hoc test was used when appropriate. Statistical significance was set at $P < 0.05$.

1. Tripodi M, Filosa A, Armentano M, Studer M (2004) The COUP-TF nuclear receptors regulate cell migration in the mammalian basal forebrain. *Development* 131(24): 6119–6129.

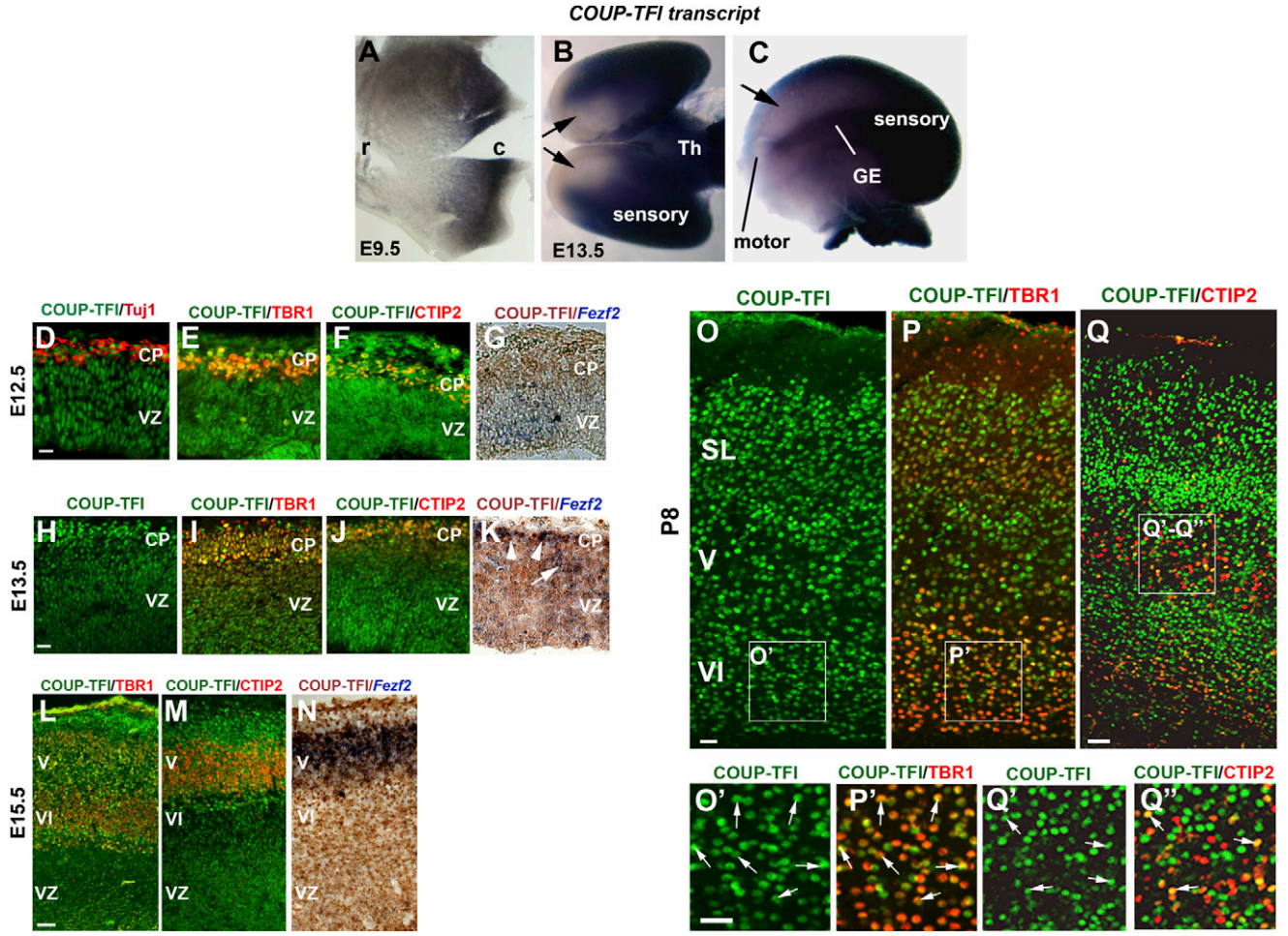

Fig. S1. COUP-TFI expression during normal corticogenesis in somatosensory cortex. (*A* and *B*) Dorsal and (*C*) latero-medial views of whole-mount preparations of the dorsal telencephalic vesicles hybridized with a *COUP-TFI* RNA probe indicate regionalized caudal expression already at E9.5. In *A*, a single vesicle was flattened to better show COUP-TFI expression. At E13.5 during CSMN specification, COUP-TFI shows a very strong caudo-lateral expression in presumptive sensory areas, and weak rostro-medial expression in presumptive motor cortex (*black arrows*). (*D–N*) Details of the presumptive somatosensory cortex double-labeled with the indicated markers at the indicated developmental stages. (*G*, *K*, and *N*) Double in situ hybridization/immunohistochemistry of *Fezf2* transcript (*blue*) and COUP-TFI protein (*brown*). (*D–G*) At E12.5, all postmitoic neurons labeled by Tuj1 (*D*), TBR1 (*E*), and CTIP2 (*F*), coexpress COUP-TFI in the nascent cortical plate (CP), whereas only few *Fezf2*-positive cells are detected in the ventricular zone (VZ). At E13.5, during CSMN differentiation, COUP-TFI expression is higher in postmitoic neurons (*H*) than in progenitors. (*K*) Colocalization of COUP-TFI protein with *Fezf2* transcript is more evident in postmitotic neurons (*arrowheads*) than in progenitor cells (*arrow*). (*I–N*) At E13.5 and E15.5, almost all TBR1- (*I* and *L*), CTIP2- (*J* and *M*), and Fezf2- (*K* and *N*) positive cells coexpress COUP-TFI in postmitotic neurons. (*O–Q″*) However, at P8 when corticogenesis is terminated, COUP-TFI is expressed at different levels within the radial extent of the somatosensory cortex (*O*) and within the same layer (*O′*). While many double COUP-TFI/TBR1-positive cells are detected in layer VI corticothalamic neurons (*P* and *P′*), in layer V only few CTIP2-positive cells coexpress COUP-TFI (*arrows* in *Q′* and *Q″*). (*O′–Q″*) High magnifications of layers V and VI taken from the boxes indicated in (*O–Q*). *Q′* shows expression of only COUP-TFI. White arrows indicate double-labeled cells. GE, ganglionic eminence; SL, superficial layers; Th, thalamus. [Scale bars: 20 μm (*D–K* and *O–Q″*); 50 μm (*L–N*).]

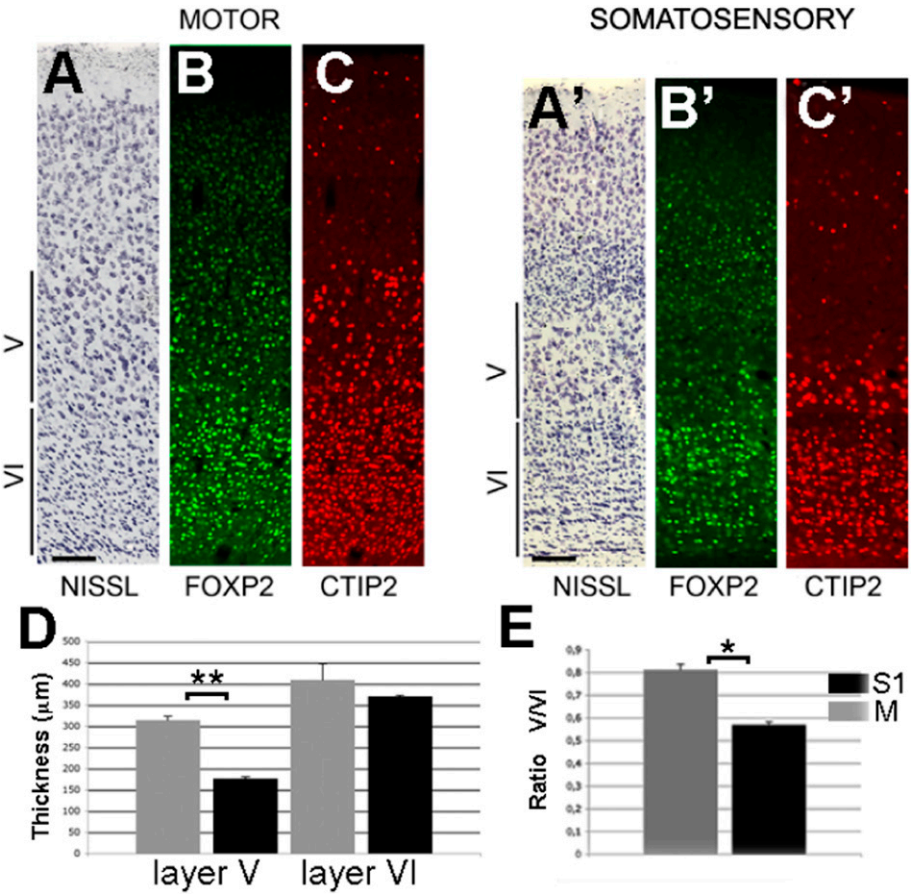

Fig. S2. Histological and molecular differences between motor and somatosensory areas in *WT* neocortex. (*A* and *A′*) Nissl staining of motor (*A*) and somatosensory (*A′*) areas of 4-week-old *WT* mice. (*B*–*C′*) Immunofluorecence of the layer VI marker FOXP2 and the layer V marker CTIP2 in motor (*B* and *C*) and somatossensory (*B′* and *C′*) areas of 4-week-old *WT* mice. (*D*) Graphical representation of the thickness of layers V and VI of motor (M) and somatosensory (S1) areas (mean ± SEM). Thickness of layer V in M is significantly bigger than layer V in S1 ($P = 0.007$; $n = 3$), whereas there is no differences in the thickness of layer VI between M and S1. (*E*) Graphical representation of the ratio between layers V and VI cell numbers (mean ± SEM) indicates a significant higher thickness of layer V in motor cortex ($P = 0.02$; $n = 3$), which is consistent with a role for COUP-TFI in delaying the onset of layer V neuron generation in somatosensory cortex during development. (Scale bars: 100 mm.)

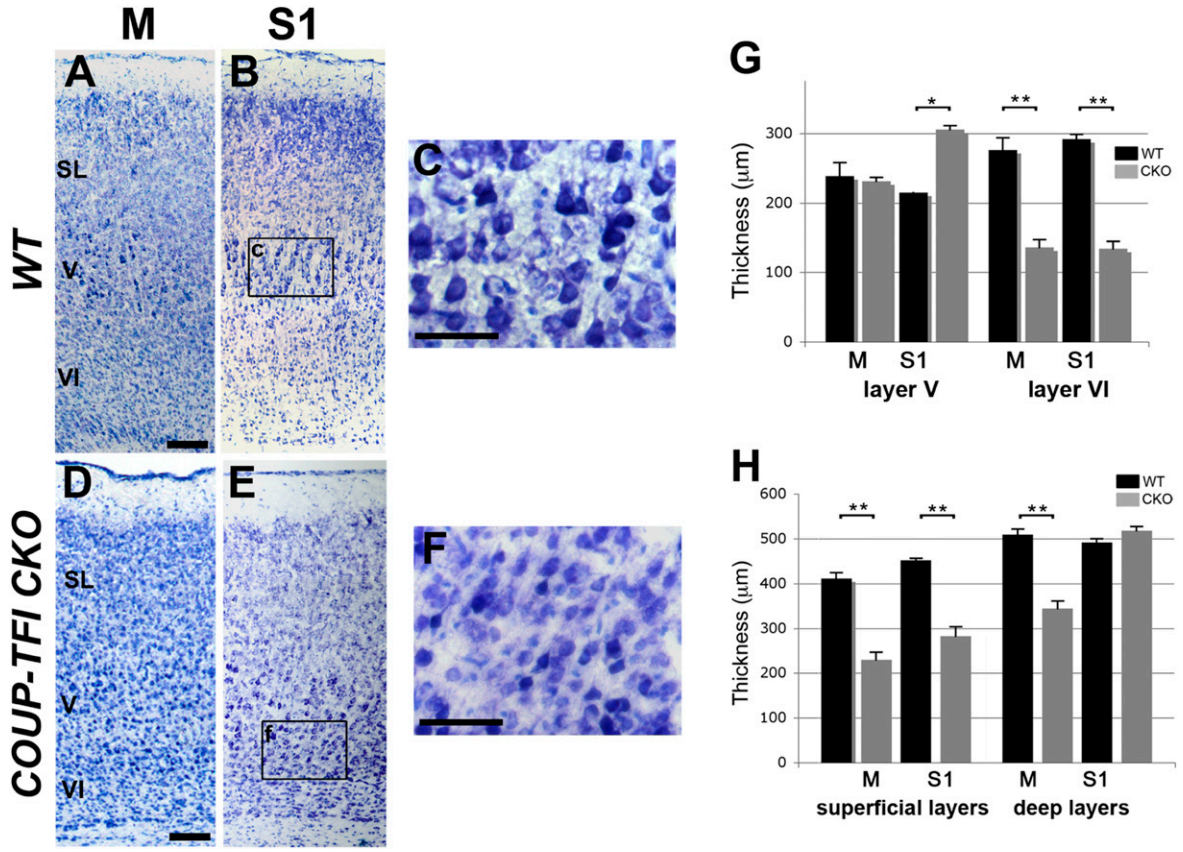

Fig. S3. Large-sized pyramidal neurons have abnormal morphology, and layer V is abnormally expanded in *COUP-TFI CKO* somatosensory cortex. (*A–E*) Nissl staining of coronal sections of *WT* and *COUP-TFI CKO* P8 brains in frontal/motor (M) and somatosensory (S1) cortical areas. (*C* and *F*) Higher magnification views of *WT* and *COUP-TFI CKO* brains in S1 taken from the boxes in (*B* and *E*). Note the reduced size and abnormal morphology of large-sized pyramidal projection neurons in *F*. (*G* and *H*) Quantification of layer and cortical thickness in *WT* (*black*) and *COUP-TFI CKO* (*gray*) P8 mice (error bars indicate SEM). (*G*) In *COUP-TFI CKO* mice, there is an expansion of layer V in S1, but not in M cortex, compared to *WT* brains (motor*: WT*, 251± 19 μm; *CKO*, 231 ± 6 μm; $n = 3$; $P = 0.4$; *S1: WT*, 215 ± 10 μm; *CKO*, 305 ± 6 μm; $P < 0.001$). In contrast to these area- and layer-specific effects, the thickness of layer VI is uniformly reduced in motor and S1 cortices (motor*: WT*, 276 ±18 μm; *CKO*, 136 ± 12 μm; $P < 0.001$; *S1: WT*, 292 ± 7 μm; *CKO*, 134 ± 11 μm; $n = 3$, $P < 0.001$). (*H*) The thickness of superficial cortical layers (SL; layers II/III and IV) is evenly decreased across cortical areas (motor*: WT* 411 ± 13 μm, *CKO* 230 ± 16 μm, $P < 0.001$; *S1: WT* 452 ± 5 μm, *CKO* 283 ± 21 μm, $n = 3$, $P < 0.001$), while deep layers (VI and V) are significantly reduced in thickness in motor, but not in S1 cortex (motor*: WT*, 509 ±13 μm, *CKO*, 344 ± 17 μm, $P < 0.001$; *S1: WT*, 491 ± 8 μm, *CKO* 518 ± 9 μm, $n = 3$, $P = 0.06$), with striking expansion of layer V in S1 of *COUP-TFI CKO* mice. [Scale bars: 500 μm (*A* and *D*); 200 μm (*B–F*).]

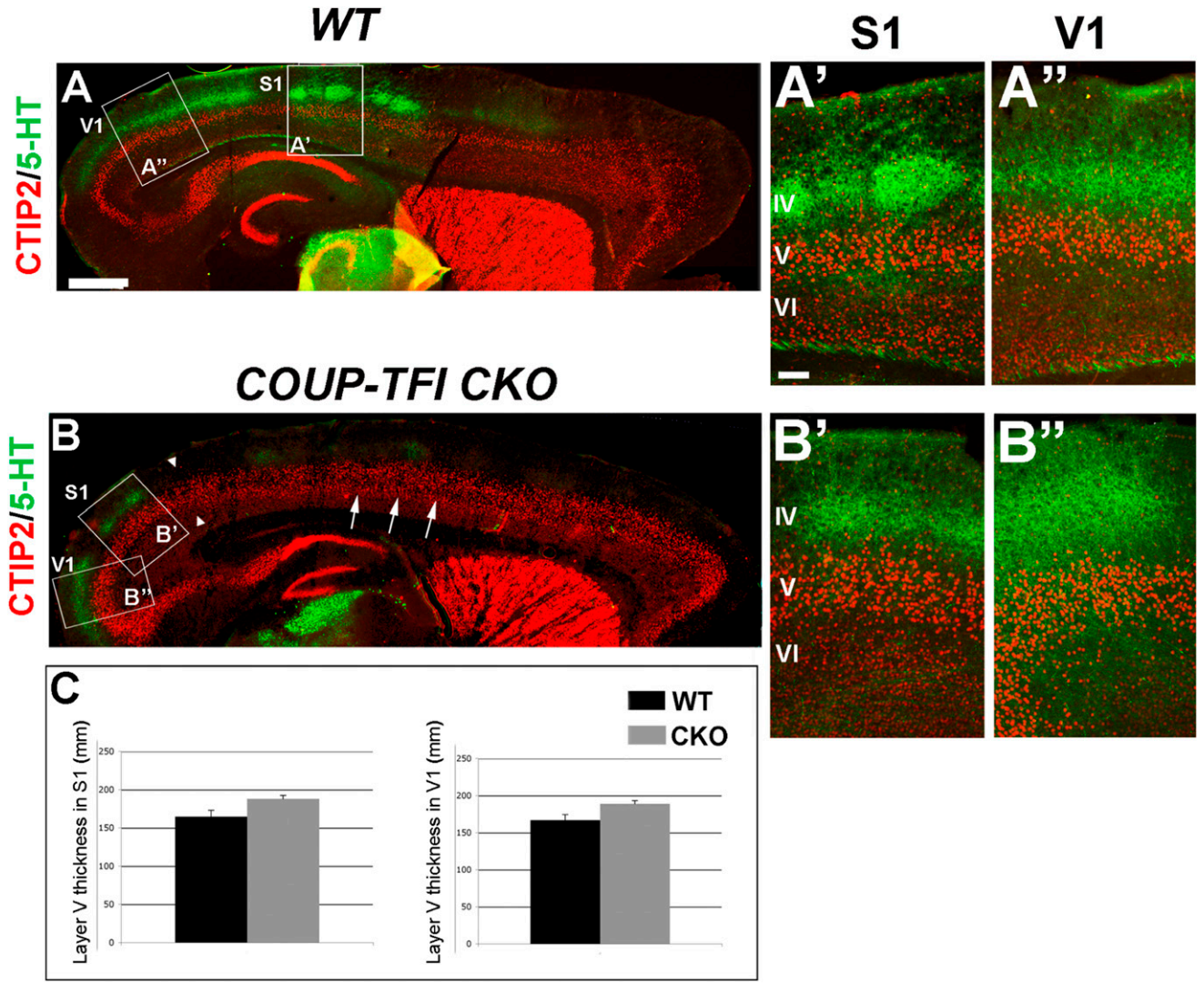

Fig. S4. Overall normal thickness of layer V in genuine sensory areas of *COUP-TFI CKO* cortices. (*A* and *B*) Double immunofluorescence with CTIP2 (*red*) and serotonin (5-HT; *green*) in P8 *WT* (*A*) and *COUP-TFI CKO* (*B*) sagittal sections. Arrows in *B* indicate radial extension of CTIP2-positive cells toward layer VI in the motorized parietal cortex. Arrowheads in *B* show that this expansion stops abruptly at the level of S1, where 5-HT labels the caudally shifted somatosensory barrel field in layer IV. (*A′*–*B″*) High magnification views of somatosensory (S1) and visual (V1) areas indicate that the overall thickness of the CTIP2-positive domain is not altered in genuine sensory areas of *WT* and *COUP-TFI CKO* cortices. (*C*) Histogram indicating that there are no significant differences in the thickness of CTIP2-positive layer V neurons in both sensory ($P = 0.07$, $n = 3$) and visual ($P = 0.06$, $n = 3$) areas of the *COUP-TFI* mutant cortex. [Scale bars: 500 mm (*A* and *B*); 100 mm (*A′* and *B′*).]

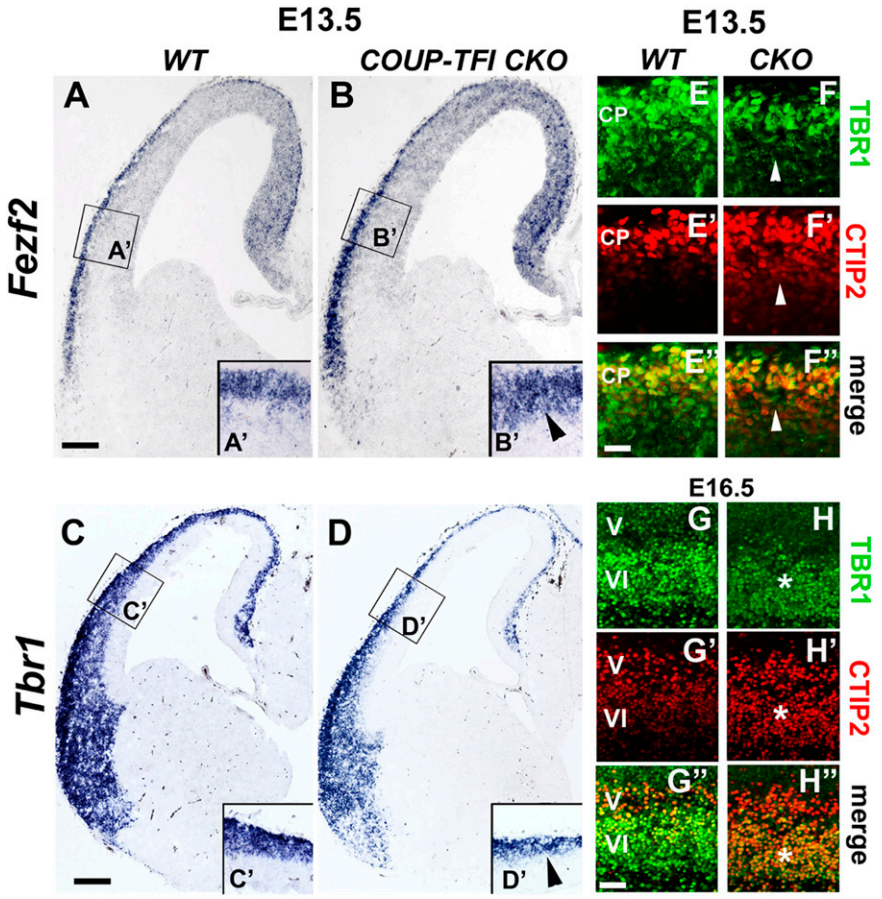

Fig. S5. Abnormal specification of layer V and VI neurons during corticogenesis in the absence of COUP-TFI. (*A–D′*) In situ hybridization on adjacent coronal sections from *WT* and *COUP-TFI CKO* E13.5 telencephalons indicates up-regulation of *Fezf2* (*B* and *B′*) and down-regulation of *Tbr1* (*D* and *D′*) in presumptive lateral cortex of *COUP-TFI CKO* embryos (*arrowheads* in *B′* and *D′*). (*E–F″*) Details of lateral cortex of adjacent sections to *A* to *D* immunostained for TBR1 and CTIP2 demonstrate decreased TBR1 and increase CTIP2 expression (*arrowheads* in *F–F″*) in the cortical plate (CP) of *COUP-TFI CKO* telencephalons. (*G–H″*) Details of lateral cortex of E16.5 brains show similarly decreased expression of TBR1 and increased expression of CTIP2 (asterisks in *H–H″*) in layers V and VI of *COUP-TFI CKO* cortices. [Scale bars: 200 μm (*A–D*); 50 μm (*E–F″*); 50 μm (*G–H″*).]

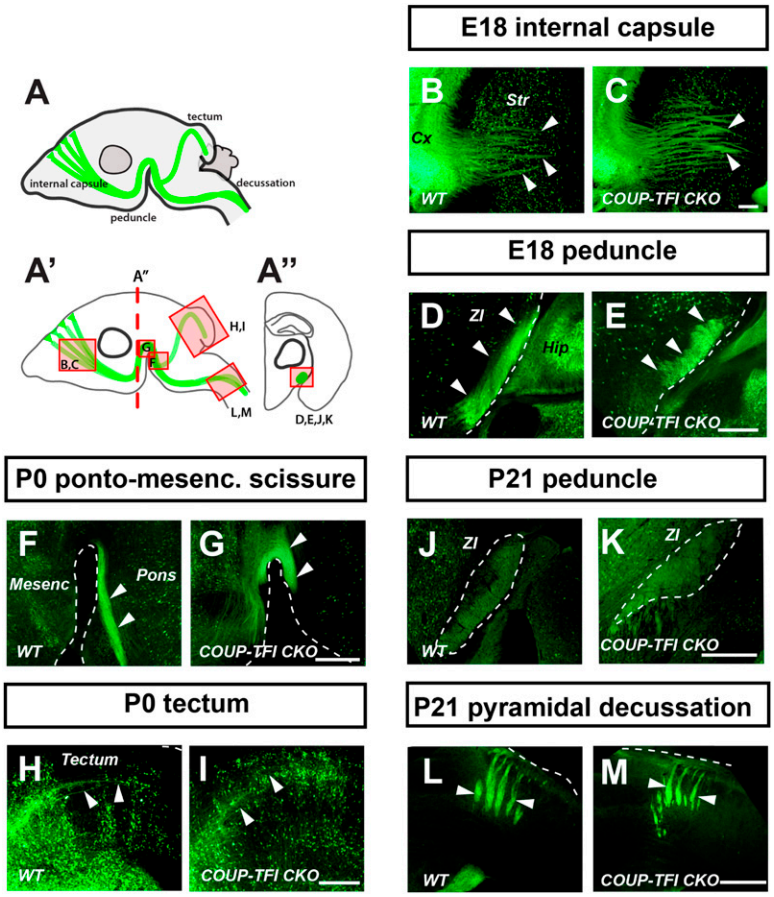

Fig. S6. Development of cortico-subcerebral connectivity in *COUP-TFI CKO* brains. (*A*–*A*″) Schematic sagittal (*A* and *A*′) and coronal (*A*″) of the brain indicating (*A*) key anatomical structures along the corticospinal/corticotectal pathways and (*A*′ and *A*″) location of the photomicrographs shown in *B* to *M*. Dashed red line in *A*′ indicates location of the coronal section depicted in *A*″. *B* to *M* are immunofluorescence photomicrographs obtained in *CST-YFP WT* and *COUP-TFI CKO* mice, highlighting cortico-subcerebral axons. At E18, corticofugal axons in *COUP-TFI CKO* mice and *WT* mice (*B* and *C*, *arrowheads*) have normal projections into the internal capsule and fasciculate compactly within the cerebral peduncles (*D* and *E*, *dashed line* indicates lateral border of the diencephalons; *arrowheads* outline medial limit of the cerebral peduncle). (*F*–*I*) At P0, subcerebral projecting axons in *COUP-TFI CKO* are appropriately fasciculated at the cerebral peduncle (*F* and *G*, *dashed line* indicates ventral border of the diencephalon and pons) and in the tectum (*H* and *I*: *arrowheads*). (*J*–*M*) At P21, corticospinal axons in *COUP-TFI CKO* are properly fasciculated at the cerebral peduncle (*J* and *K*, *arrowheads*; *dashed line* indicates ventral limit of the ponto-mesencephalic scissure) and decussate normally in the medulla oblongata (*L* and *M*, *arrowheads*). Cx, cortex; Hip, hippocampus; Mesenceph, mesencephalon; Str, striatum; ZI, zona incerta. (Scale bars: 250 μm.)

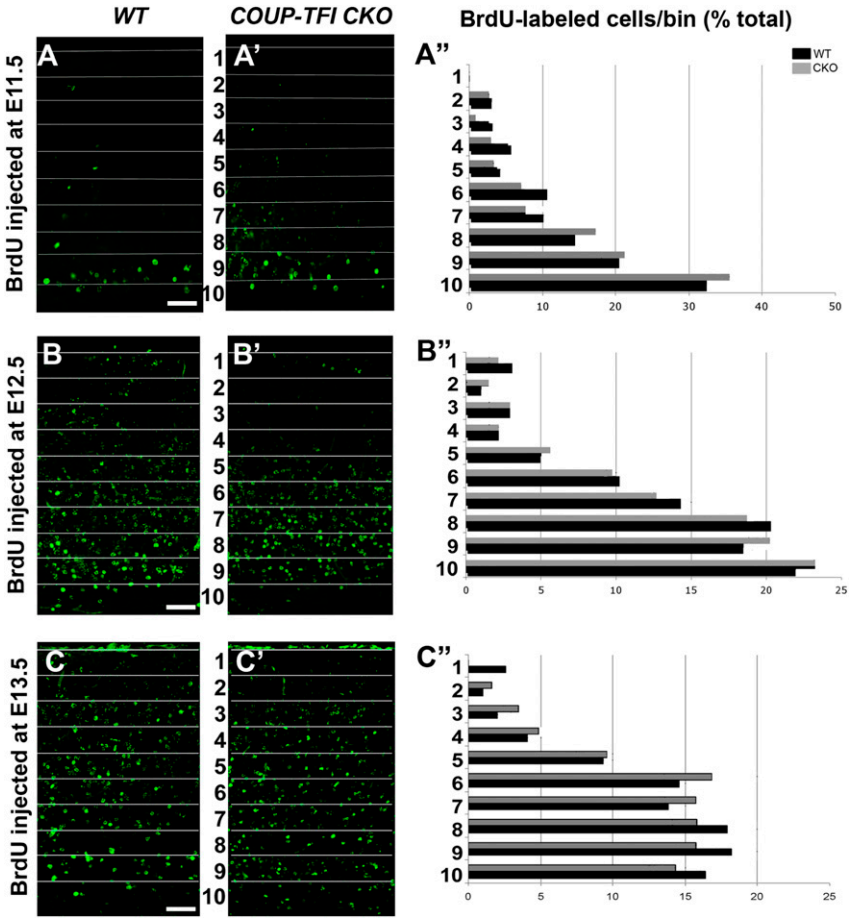

Fig. S7. Normal migration of early-born neurons in *COUP-TFI CKO* brains. (*A*–*C*′) Representative photomicrographs of P0 coronal sections from somatosensory cortex after BrdU injection at E11.5 (*A* and *A*′), E12.5 (*B* and *B*′), and E13.5 (*C* and *C*′) in *WT* and *COUP-TFI CKO* brains. The cortical thickness was divided radially into 10 equal bins and the distribution of BrdU-labeled cells across the bins was determined. (*A*″–*C*″) Percentages of BrdU birth-dated cells in each bin show similar distribution of BrdU-labeled neurons between *WT* and *COUP-TFI CKO* mice for all stages examined. (Scale bars: 100 μm.)

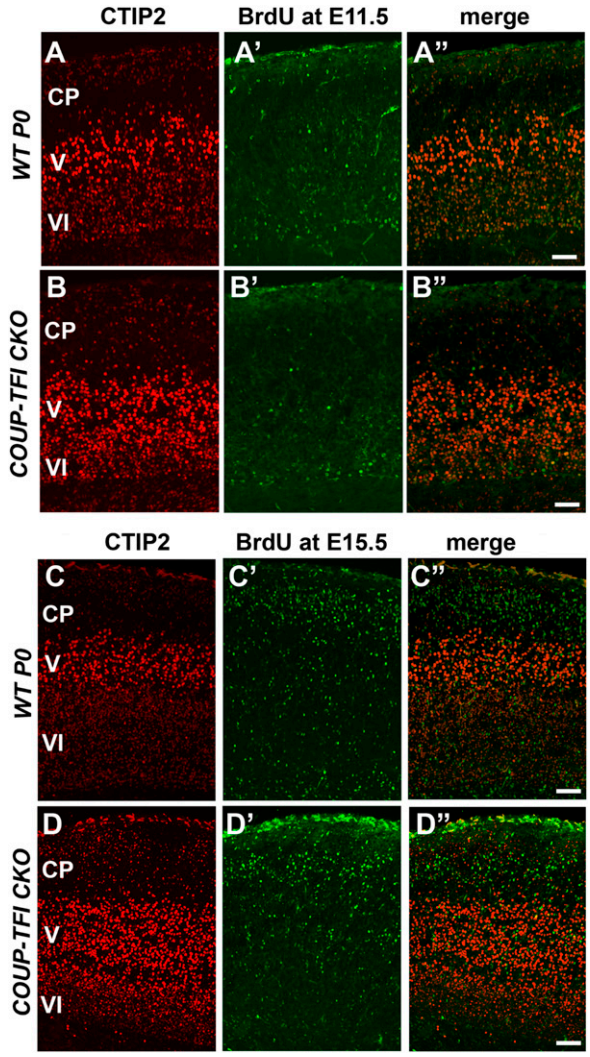

Fig. S8. CTIP2-positive neurons in layer VI are not born when subplate or superficial layer neurons are generated in *COUP-TFI CKO* brains. (*A–D″*) Coronal sections of P0 *WT* and *COUP-TFI CKO* parietal cortices after BrdU injection at E11.5 (*A–B″*) and E15.5 (*C–D″*), and immunostained for BrdU and CTIP2. CTIP2-positive neurons are overwhelmingly not labeled by BrdU injected at E11.5 or E15.5, indicating that abnormally CTIP2-expressing neurons of layer VI are largely not being generated at E11.5 and E15.5 in *COUP-TFI CKO* mice. (Scale bars: 50 μm.)

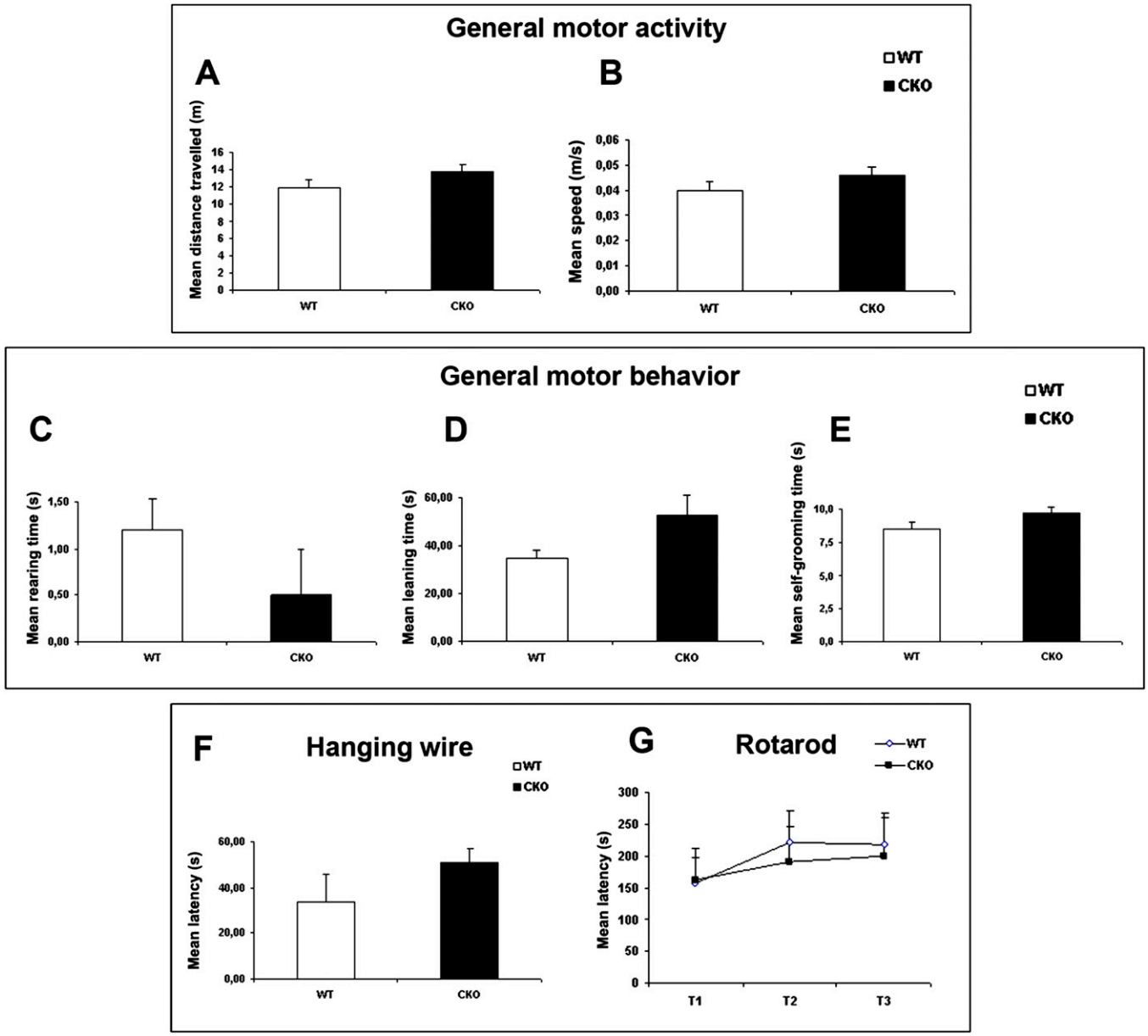

Fig. S9. General motor function is not impaired in *COUP-TFI CKO* adult mice. (*A–E*) Mean values with SEM of measures analyzed during 5 min recording of motor activity in a novel cage in *WT* and *COUP-TFI CKO* mice. (*A*) Distance traveled (m). (*B*) Mean speed (m/s). (*C*) Rearing time (s). (*D*) Leaning time (s). (*E*) Self-grooming time (s). There are no significant differences in these values between *WT* and *COUP-TFI CKO* mice. (*F* and *G*) Mean latency to fall off during the single trial hanging wire task (*F*) and the three consecutive trials rotarod test (*G*) in *WT* and *COUP-TFI CKO* mice. No significant differences are detected between *WT* and *COUP-TFI CKO* mice.

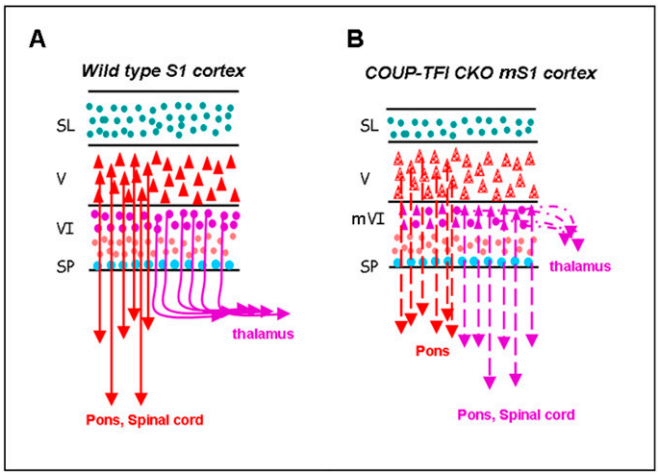

Fig. S10. Model of the role of COUP-TFI in regulating CSMN differentiation. (*A* and *B*) Schematic diagram showing the cellular and morphological changes occurring in the absence of COUP-TFI function. (*A*) Red triangles indicate large pyramidal CSMN in layer V projecting toward the pons and spinal cord, whereas corticothalamic layer VI neurons (*round-shaped purple circles*) project toward the thalamus in *WT* S1 cortex. (*B*) Genuine CSMN differentiate abnormally (*patterned red triangles*) and project only as far as the pons in *COUP-TFI CKO* mice, whereas aberrantly differentiated neurons located superficially in layer VIa (mVI; *small purple triangles*) project abnormally toward subcerebral targets in the pons and spinal cord. Small pink circles indicate layer VIb neurons. Large blue circles indicate subplate neurons (SP). The thickness of superficial layers (SL) is decreased in *COUP-TFI CKO* mice.

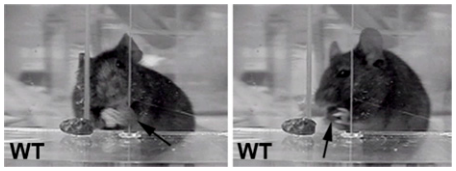

Movie S1. Skilled reaching-task procedure in *WT* and *COUP-TFI CKO* mice. Adult mice are required to grasp food pellets through an indentation, which requires the use of their forelimb paws. The trial ended when 20 pellets were retrieved or 10 min passed. Movie S1 shows the performance of a *WT* mouse, which grasps the food pellet very quickly and presents it to the mouth with the help of its paws.

Movie S1

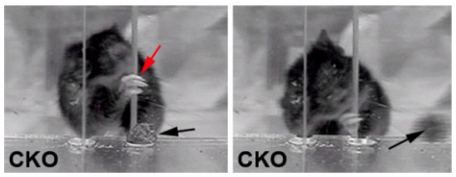

Movie S2. Performance of a typical *COUP-TFI CKO* mouse. In this case, the mouse fails to lift the paw properly, performs a misguided reach, and fails to retrieve the food pellet after various unsuccessful attempts.

Movie S2